Curcumol Inhibits Lung Adenocarcinoma Growth and Metastasis via Inactivation of PI3K/AKT and Wnt/β-Catenin Pathway

Sheng Li,*[1] Guoren Zhou,*[1] Wei Liu,† Jinjun Ye,† Fangliang Yuan,‡ and Zhi Zhang‡

*Department of Chemotherapy, Jiangsu Cancer Hospital and Jiangsu Institute of Cancer Research
and Nanjing Medical University Affiliated Cancer Hospital, Nanjing, P.R. China
†Department of Radiotherapy, Jiangsu Cancer Hospital and Jiangsu Institute of Cancer Research
and Nanjing Medical University Affiliated Cancer Hospital, Nanjing, P.R. China
‡Department of Thoracic Surgery, Jiangsu Cancer Hospital and Jiangsu Institute of Cancer Research
and Nanjing Medical University Affiliated Cancer Hospital, Nanjing, P.R. China

Curcumol (Cur), isolated from the Traditional Chinese Medical plant *Rhizoma Curcumae*, is the bioactive component of sesquiterpene reported to possess antitumor activity. However, its bioactivity and mechanisms against lung adenocarcinoma are still unclear. We investigated its effect on lung adenocarcinoma and elucidated its underlying molecular mechanisms. In vitro, Cur effectively suppressed proliferation, migration, and invasion of lung adenocarcinoma cells A549 and H460, which were associated with the altered expressions of signaling molecules, including p-AKT, p-PI3K, p-LRP5/6, AXIN, APC, GSK3 and p-β-catenin, matrix metalloproteinase (MMP)-2, and MMP-9. Furthermore, Cur significantly induced cell apoptosis of A549 and H460 by promoting the expression of Bax, caspase 3, and caspase 9 and suppressing the expression of Bcl-2, and arrested the cell cycle at the G_0/G_1 phase by lowering the levels of cyclin D1, CDK1, and CDK4. In vivo experiment revealed that Cur could inhibit lung tumor growth and lung metastasis, which were consistent with these in vitro results. In xenograft model mice, Cur strongly decreased tumor weight and tumor volume, which may be related to the downregulation of p-AKT and p-PI3K by immunofluorescence analysis. In addition, a lung metastasis model experiment suggested that Cur dramatically decreased the ratio of lung/total weight, tumor metastatic nodules, and the expressions of MMP-2 and MMP-9 in lung tissues compared with the control. Overall, these data suggested that the inhibitory activity of Cur on lung adenocarcinoma via the inactivation of PI3K/Akt and Wnt/β-catenin pathways, at least in part, indicates that curcumol may be a potential antitumor agent for lung adenocarcinoma therapy.

Key words: Curcumol; Lung adenocarcinoma; Proliferation; Metastasis; PI3K/AKT; Wnt/β-catenin

INTRODUCTION

Lung cancer is the predominant cause of cancer-related mortality and is ranked among the cancers with the lowest rates of 5-year survival[1,2]. Non-small cell lung cancer (NSCLC), accounting for about 80–85% of all lung cancers[3–5], is mostly found in the middle and late stages, and the 5-year survival rate is very low. Lung adenocarcinoma is the most diagnosed histological subtype of NSCLC with high morbidity and mortality[6,7]. There are a lot of limitations in the usual way to treat NSCLC[8,9]. Although many recent advances have been made in the diagnosis and treatment of tumors, the efficient treatments for lung adenocarcinoma remain insufficient[10]. For example, the resection of tumor causes systemic inflammation and may disseminate cancer cells into the blood, which promote the metastasis of cancer[8,11]. In addition, the prognosis of lung adenocarcinoma after surgery is troubling, with poor response rates, severe toxicities, and high recurrence rates[12,13]. Therefore, developing more agents to supplement the deficiencies of conventional treatment for cancer is urgent.

Natural products have been the subject of many drug discovery efforts[14]. In Asian countries, herbal medicines have special clinical significance without altering their basic therapeutic features and are the natural sources of biologically active compounds. Curcumol (Cur, $C_{15}H_{24}O_2$, the chemical structure is shown in Fig. 1A), a sesquiterpene
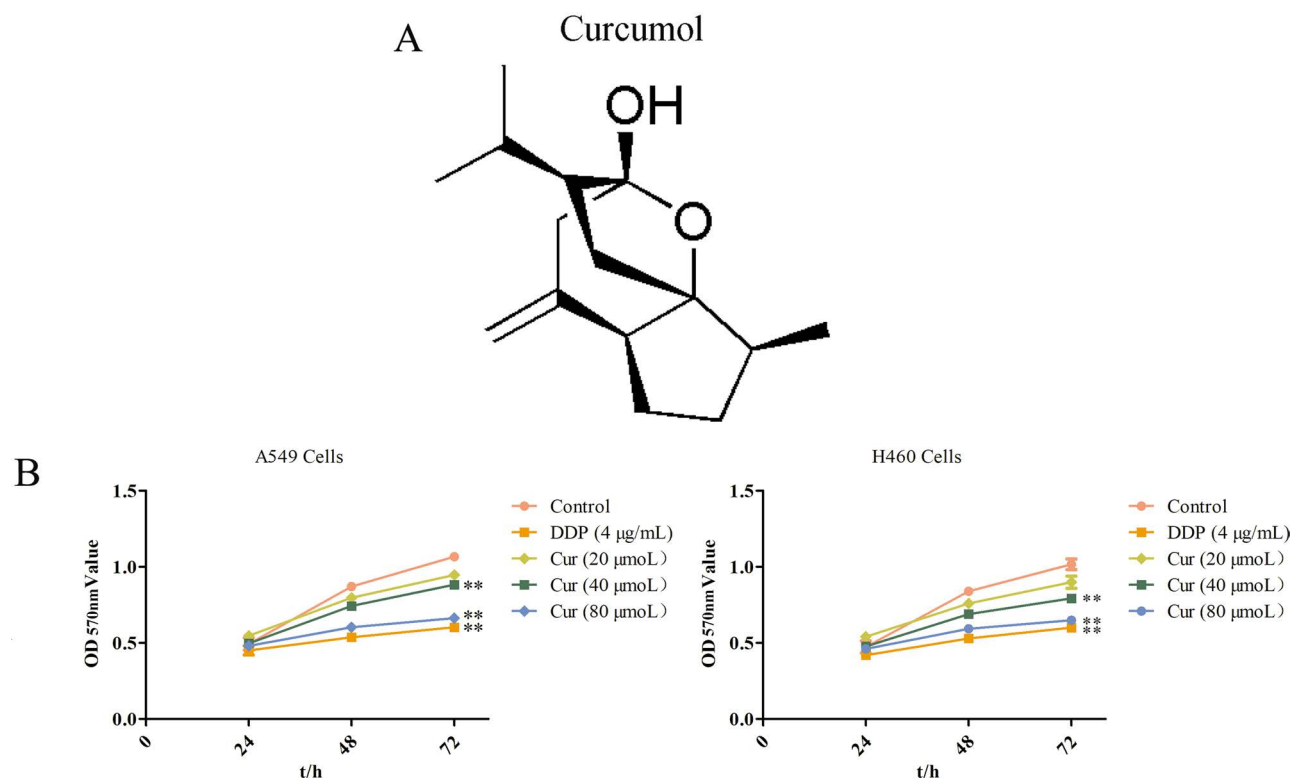

Figure 1. (A) The chemical structure of curcumol (Cur). (B) Cur inhibited proliferation of A549 and H460 cells. Exponentially growing cells were treated with different concentrations of Cur (20, 40, and 80 μmol/L) for 24, 48, and 72 h, and then cell proliferation was measured by MTT assay. Data are shown as the mean $\pm$ SD. ** $p < 0.01$ versus control group.

isolated from the traditional Chinese medicinal herb *Rhizoma Curcumae*, has been reported to have potent anti-tumor activity[15]. It effectively inhibited the occurrence of skin cancer, gastric cancer, duodenal cancer, colon cancer, and breast cancer in the experimental animals and reduced the number of tumors and tumor size[16,17]. Although Cur and its bioactivity had been reported by many researchers, the activities and mechanisms against lung adenocarcinoma are still unclear. Thus, this study was conducted to discover the inner effect and mechanisms of Cur on lung adenocarcinoma cell lines A549 and H460 in vitro and in vivo. We found that Cur inhibited proliferation and metastasis of lung adenocarcinoma by inhibiting PI3K/Akt and Wnt/ -catenin pathways.

MATERIALS AND METHODS

Chemicals

Curcumol (lot: 100185-200506) was obtained from the National Institute for the Control of Pharmaceutical and Biological Products (Beijing, China). 3-(4, 5)-Dimethylthiahiazo(-z-y1)-2,5-diphenytetrazolium bromide (MTT) and dimethyl sulfoxide (DMSO) were purchased from Amerso Chemical Co. (St. Louis, MO,

USA). Propidium iodide (PI) and Annexin-V–FITC apoptosis detection kit were purchased from BD Biosciences (Bedford, MA, USA). 4 ,6-Diamidino-2-phenylindole dihydrochloride (DAPI) was purchased from Kaiji Biotechnology (Santa Cruz, CA, USA).

Cell Culture and Proliferation

Human lung cancer A549 and H460 cell lines were purchased from Shanghai Institute of Cell Biology in the Chinese Academy of Sciences (Shanghai, China) and cultured in DMEM supplemented with 10% FBS at a humidified atmosphere (95% air, 5% CO_2, 37°C). MTT assay was used to detect cell proliferation according to the manufacturer's instructions (Roche Applied Science, Indianapolis, IN, USA). Briefly, approximately 1×10^5 cells were seeded in 96-well plates (Corning, New York, NY, USA) for 24, 48, and 72 h at 37°C and then exposed to designated doses of the various drug concentrations [Cur 20, 40 80, 100, and 120 μmol/L and cisplatin (DDP), positive drug, 4 μmol/L] followed by 5 mg/ml of MTT solution. Optical density (OD) was recorded with a 96-well microplate reader (Bio-Rad Laboratories, Hercules, CA, USA) at 570 nm. Data represent at least three separate experiments.

Morphology Analysis

A549 and H460 cells were seeded into 24-well plates (1×10^4 cells per well), and these cells were exposed to different concentrations of Cur (20, 40, and 80 µmol/L) for 24 h. The cell morphology was observed under inverted light microscopy (BX41; Olympus Optical Co., Tokyo, Japan). The lung cancer cell death pattern induced by Cur was evaluated using acridine orange/ethidium bromide (AO/EB solution, 100 mg/ml of AO and EB in PBS, respectively) staining.

Cell Apoptosis Detection

Cell apoptosis was determined by flow cytometer analysis using the Annexin-V–FITC apoptosis detection kit (KeyGEN, Nanjing, China) according to the manufacturer's instructions. In brief, the cells were treated with different concentrations of Cur for 48 h, and they were harvested and washed with PBS. Then cells were stained with Annexin-V–FITC and PI, and analyzed with FCM (Becton Dickinson, San Jose, CA, USA).

Cell Cycle Analysis

Cell cycle distributions were determined by PI (KeyGEN BioTECH) staining. In brief, A549 and H460 cells were harvested and suspended in 500 µl of PBS after treatment with Cur at concentrations of 20, 40, and 80 µmol/L for 24 h. After fixing (70% ethanol at 4°C for 2 h) and PI staining, cells were analyzed by FACStar flow cytometry (BD Biosciences) and calculated with Mod FIT LT 2.0 version software (BD Biosciences).

Scratch Wound Assay

Cell motility of A549 and H460 cells was assessed using scratch wound assay. Cells (1×10^5/ml) were seeded in a six-well plate and cultured in medium containing 10% FBS overnight. The cells were carefully wounded using a yellow pipette tip, and cellular debris was removed by washing with DMEM. A fresh medium with or without Cur (20, 40, and 80 µmol/L) was added to the wells, and the plate was incubated for 24 h. The crosses of each well were photographed under an Olympus IX-71 microscope at 0, 12, and 24 h, respectively. Motility was determined by the count of the migrated cells.

Transwell Invasion Assays

Transwell chambers (Corning) were used to evaluate the migration of A549 and H460 cells. Briefly, cells pretreated with or without Cur (20, 40, and 80 µmol/L) were trypsinized and resuspended with medium lacking FBS. Cells (1×10^5) were added to the upper chamber of the inserts with Matrix gel, while 600 µl of medium with 50% FBS was added to the lower chamber. The invading cells were stained by crystal violet and imaged after 30 h of culturing (magnification: 200×).

Western Blot Analysis

Cells treated with or without the Cur (20, 40, and 80 µmol/L) were lysed in RIPA lysis buffer on ice for 30 min. After $12,000 \times g$ centrifugation for 15 min at 4°C, the total protein concentrations of the supernatant was determined by the BCA protein assay kit (Beyotime Institute of Biotechnology, Haimen, China). Equivalent samples of cell lysates were separated using 10% SDS-PAGE and then transferred onto a PVDF membrane for 2 h. The membranes were blocked with 5% nonfat skim milk in TBST buffer at room temperature for 1 h and incubated with the following primary antibodies at 4°C overnight: -actin, Bax, Bcl-2, caspase 3, caspase 9, cyclin A, cyclin B1, cyclin D1, cyclin E, CDK1, CDK2, CDK4, MMP-2, MMP-9, pI3K, pAKT, tAKT, LRP5/6, p-LRP5/6, Frizzled8, AXIN1, APC, GSK3 , p- -catenin, and -catenin. The proteins were detected by Quantity One software on a GS-800 densitometer (Bio-Rad Laboratories). All data were normalized to the mean value of the control group (-actin).

Animal Model

Animal studies were approved by the Institutional Animal Care and Use Committee at the Nanjing Medical University (Nanjing, China). The BALB/c female nude mice ($N = 100$, 6 weeks old, 18–22 g) were housed in steel microisolator cages at 22°C with a 12/12-h light/dark cycle and freely received a standard mouse chow and tap water.

Xenograft Model. After being anesthetized by inhalation, mice were inoculated with the A549 cells (100 µl of 1×10^6 cells) into the right armpit once a day. The mice were randomized into Control (PBS, phosphate buffer saline), Cur (100, 200, and 300 mg/kg), and cisplatin (DDP, positive, 1 mg/kg) groups of six animals when xenografts were palpable with an average size of 50–70 mm³. These five groups were administered p.o. every day until sacrifice. Twenty-one days after treatment, the mice were humanely sacrificed, and the body weight of each animal, and the morphology, volume, and weight of the tumors were monitored. Furthermore, lung tissues were collected and excised for immunohistochemistry and immunofluorescence analysis.

Pulmonary Metastasis Model. Mice were injected 100 µl of 1×10^6 A549 cells into the median tail vein once a day. One week later, the mice were randomized into Control (PBS, phosphate buffer saline), Cur (100, 200, and 300 mg/kg), and cisplatin (DDP, positive, 1 mg/kg) as positive control. The mice in Control and Cur groups were administered p.o. every day until sacrifice, and the mice in the DDP group were injected with DDP (1 mg/kg) intraperitoneally in accordance with the body weight, once a day until sacrifice. Then mice were sacrificed on day 21, and the lungs were removed and weighed.

TUNEL Staining

TUNEL staining of paraffin-embedded tumor sections demonstrated apoptosis (Beyotime Institute of Biotechnology). In brief, cells were fixed with 10% formalin at 37°C for 1 h, and groups of slips were incubated in permeabilization solution (1% Triton X-100 in PBS, freshly prepared) for 10 min on ice. After washing with PBS three times, the slides were incubated with TUNEL working solution in a humidified chamber at 37°C for 1 h. Samples were counterstained with DAPI in room temperature for 5 min and examined under a light microscope (Olympus Corp). TUNEL-positive cells in four random fields were counted and analyzed with GraphPad Prism software (version 5.0) for each group (magnification: 200×).

Immunohistochemical and Immunofluorescence Analysis

Tumor specimens from the BALB/c nude mice were immunohistochemically stained for Ki-67 using previously reported protocols[18]. Tumor samples stained for apoptosis protein (Bax, Bcl-2, caspase 3, caspase 9) and PI3K, AKT, and -catenin protein were analyzed by immunohistochemical or immunofluorescence methods, respectively. Briefly, tumors were fixed in 4% neutral formalin for 24 h, embedded in paraffin, and were serially sectioned at 5 μm. Sections were deparaffinized and rehydrated, then submerged in hydrogen peroxide to quench peroxidase activity following incubation with 1% BSA to block nonspecific binding sites. After incubation with primary antibody at 4°C for 12 h, secondary antibody was applied to slides for 1 h at room temperature. For immunohistochemical analysis, the slice was colored by diaminobenzidine kit (DAB; Beyotime) followed by counterstaining with hematoxylin. All the sections were visualized using DAB under a light microscope (Nikon 80 i). For immunofluorescence analysis, the nuclei were counterstained using DAPI (Invitrogen, Carlsbad, CA, USA) before they were mounted with ProLong Gold antifade reagent (Invitrogen). Fluorescence cells were examined and captured under an inverted fluorescence microscope.

Histological Assay

The lung tissues were obtained and fixed in 10% formalin and then stained by hematoxylin eosin staining. Ten random areas of interest were examined in each section and were identified by computer-generated field identification. At least six different sections of lung tissues were examined for each animal in groups. Images were obtained using a fluorescence microscope.

Statistics

Data analyses were performed using the SPSS 18.0. statistical software. Results were expressed as mean $\pm$ SD ($N=3$). Differences between groups were calculated with one-way ANOVA. A value of $p<0.05$ was considered statistically significant.

RESULTS

Curcumol (Cur) Inhibited Proliferation of A549 and H460 Cells

The growth-inhibitory effects of one compound can be evaluated by testing the ability to inhibit the proliferation of cancer cells[19]. Therefore, the effect of Cur (20, 40, and 80 μmol/L) on the proliferation of A549 and H460 cells at 24, 48, and 72 h was estimated using MTT assay. The results demonstrated that the viability of A549 and H460 cells was obviously lessened with the increase in Cur concentration (Fig. 1B). Taken together, Cur significantly inhibited the A549 and H460 cell proliferation in a dose- and time-dependent manner.

Cur Induced Apoptosis of A549 and H460 Cells

Most cancer cells block apoptosis, causing the survival of malignant cells despite genetic and morphologic transformations. The development of agents that effectively induce apoptosis in cancer cells has been regarded as an important goal in cancer research and therapy[20]. In order to determine whether Cur-mediated anticancer activity in lung adenocarcinoma cells was associated with the induction of apoptosis, the A549 and H460 cells were incubated with Cur (20, 40, and 80 μmol/L) for 24 h and then visualized by light microscopy. As shown in Figure 2A, the results revealed that treatment with Cur (40 and 80 μmol/L) resulted in protuberant cytoplasmic blebs and progressive shrinkage in both A549 and H460 cells.

Apoptotic cells exhibit increased plasma membrane permeability to certain fluorescent dyes, which allows apoptosis-associated biochemical changes in the DNA. These were observed on the cell surface. Microscopic examination of A549 and H460 cells after Cur treatment was recommended as the most reliable method to distinguish viable, early, or late apoptotic and necrotic cells. A distinct phenomenon of apoptosis was observed on Cur-treated cells (Fig. 2B), and with the increasing concentration of the Cur, early apoptotic cells (EA), late apoptotic cells (LA), and necrotic cells (N) appeared sequentially. Furthermore, Cur (40 and 80 μmol/L) had a better effect on H460 than A549 cells.

To confirm the quantity of cell death, Annexin-V–FITC/PI dual staining was performed by flow cytometry. As shown in Figure 2C, when A549 and H460 cells were treated with 20, 40, and 80 μmol/L of Cur for 24 h, the apoptotic rate was significantly increased in lung cancer cells, especially in A549 cells. Western blotting results indicated that Cur could increase the levels of Bax, caspase 3, and caspase 9, and decrease the antiapoptotic protein of Bcl-2 in A549 and H460 cells (Fig. 2D).

Cur Arrested Cell Cycle in A549 and H460 Cells

To gain further insights into the mechanism of the antiproliferative activity for Cur in A549 and H460 cells,
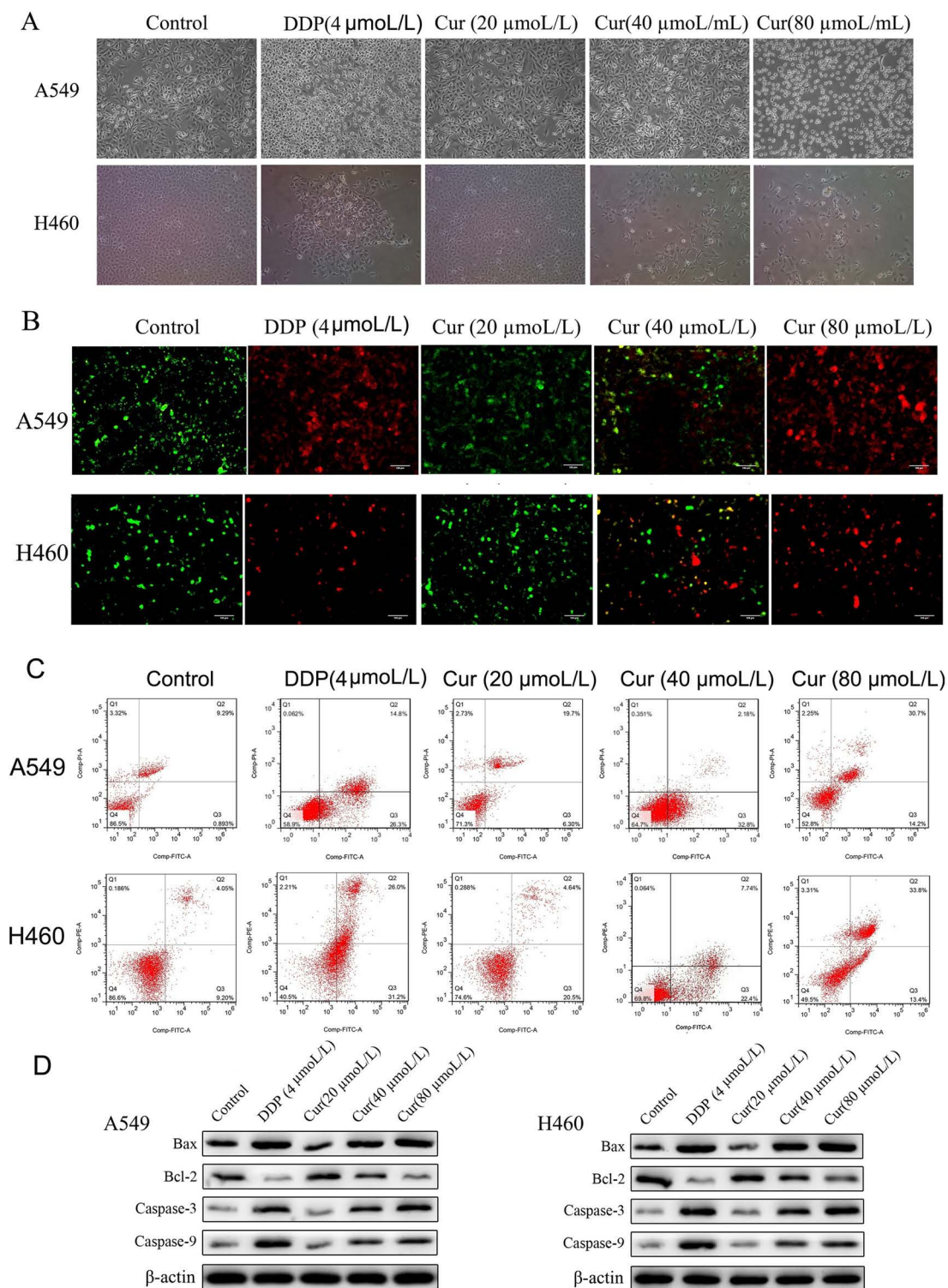
Figure 2. Cur induced the apoptosis of A549 and H460 cells treated with concentrations of 20, 40, and 80 μmol/L. (A) Morphological changes of cells (200×). (B) Morphological changes of A549 and H460 cells and analyzed by AO/EB double-staining under fluorescence microscope (200×). Live cells (L) are shown in green; apoptotic cells are shown in orange-yellow fragments (EA, early apoptotic cells as orange fragments; LA, late apoptotic cells as yellow fragments), and necrotic cells (N) are indicated as red. (C) The apoptosis rate of A549 and H460 was determined by FACS assay with Annexin-V–FITC/PI dual staining method. (D) Western blotting of Bax, Bcl-2, caspase 3, and caspase 9 proteins after 48 h of treatment with different concentrations of Cur in A549 and H460 cancer cells. Equal protein loading was evaluated by -actin.

its effects on cell cycle distribution were analyzed using flow cytometry. As shown in Figure 3A, the treatment of A549 and H460 cells with Cur (80 μmol/L) caused an obvious increase in the proportion of cells in the G_0/G_1 phase (15.01% and 19.32% at 24 h, respectively), which was accompanied by a corresponding reduction in the percentage of cells in the S phase (5.61% and 9.10% at 24 h) and G_2/M phase (9.41% and 10.22% at 24 h, respectively), compared with the control group. Western blotting results indicated that Cur evidently decreased the levels of cyclin D1, CDK1, and CDK4, closely related to the progress of G_0/G_1 phase, while the expression of cyclin A, cyclin B1, cyclin E, and CDK2 involved in the G_2/M or S phase had no distinct changes (Fig. 3B). These results demonstrated that Cur blocked the proliferation of A549 and H460 cells by arresting the cell cycle at the G_0/G_1 phase.

Cur Suppressed Cell Migration and Invasion of A549 and H460 Cells

The migratory and invasion ability of A549 and H460 cells was determined using the scratch wound assay and Transwell assay. The cells were cultured with different concentrations of Cur (20, 40, and 80 μmol/L) for 24 h. In the scratch wound assay, the open wound area of the cells treated with Cur at 20 to 80 μmol/L was significantly greater than that of the untreated controls, indicating that Cur significantly inhibited A549 and H460 cell migration in a dose-dependent manner (Fig. 4A). In the Transwell invasion assay, incubation of A549 and H460 cells with increasing concentrations of Cur (20, 40, and 80 μmol/L) led to a concentration and decrease in the number of invasive cells (Fig. 4B). In addition, the matrix metalloproteinases (MMPs), a group of zinc-dependent ECM-degrading enzymes, are thought to play a critical role in tumor cell invasion and migration. Thus, we assessed the levels of MMP protein by Western blotting. As a result, the expression of MMP-2, and MMP-9 protein was dose-dependently decreased in Cur-treated cells compared to the control treatment, especially in the Cur group (80 μmol/L) (Fig. 4C). These results revealed that Cur had an important role in inhibiting migration and invasion of lung adenocarcinoma cells in vitro, which may be related to the depressed levels of MMP protein.

Cur Inactivated the PI3K/AKT and Wnt/β-Catenin Signaling Pathway

PI3K/AKT and Wnt/ -catenin signaling play a crucial role in regulating cell proliferation and survival, motility and migration, and tumor cell invasion[21–22]. Thus, to confirm that the antiproliferation effects of Cur on the lung adenocarcinoma are related with the inactivation of these pathway, the effect of Cur on the PI3K/AKT and Wnt/ -catenin signal was preliminary conducted. A549 and H460 cells were stimulated with Cur (20, 40, and 80 μmol/L) for 24 h, and Western blotting analysis was used to investigate the protein expression of PI3K/AKT and Wnt/ -catenin. We found that Cur effectively reduced the phosphorylation levels of PI3K and AKT protein (Fig. 5A), indicating that curcumol could suppress the activation of PI3K and AKT in A549 and H460 cells. Cur could suppress the phosphorylation of LRP5/6, while it had no changes on Frizzled8 (Fig. 5B), and in turn significantly increased the AXIN, APC, and GSK3 protein expression (Fig. 5C). Moreover, as shown in Figure 5D, the phosphorylation level of -catenin protein was significantly increased, while the -catenin protein expression was distinctly decreased.

Cur Retarded Tumor Growth in Nude Mice

In view of the ability of Cur to inhibit lung adenocarcinoma A549 and H460 cells' proliferation and metastasis in vitro and to further understand these effect in vivo, a pulmonary xenograft model was duplicated using male nude mice. The results indicated that Cur treatment significantly inhibited tumor volume (Fig. 6A), tumor weight (Fig. 6B), and body weight loss (Fig. 6C). The tumor size in the Cur-treated group was remarkably reduced (Fig. 6D). Immunohistochemistry staining of the excised tumor sections from Cur groups (100, 200, and 300 mg/kg) showed lower expression of Ki-67, but a higher percentage of TUNEL-positive cells compared to those of the control group, suggesting that Cur could inhibit proliferation and induce apoptosis in vivo, which is consistent with the in vitro results (Fig. 6E).

In addition, immunofluorescence staining was used to determine the translocation of protein in PI3K/AKT and Wnt/ -catenin. As shown in Figure 7, Cur downregulated the expression of the phosphorylation of PI3K (p-PI3K) (Fig. 7B) and AKT (pAKT) (Fig. 7D), and had no effect on the level of PI3K (Fig. 7A) and t-AKT (Fig. 7C). Cur also dramatically blocked -catenin nuclear translocation, as indicated by the decreased expression of -catenin and elevated phosphorylation level of -catenin (p- -catenin) (Fig. 8A). Furthermore, Cur significantly increased the expression of Bax, caspase 3, and caspase 9, and downregulated the levels of Bcl-2 (Fig. 8B). These results further confirmed that Cur could also inhibit lung adenocarcinoma cell proliferation via regulation of the PI3K/AKT and Wnt/ -catenin pathway in vivo.

Cur Suppressed Tumor Metastasis in Nude Mice

The metastasis model was performed to determine the effect of Cur on lung adenocarcinoma metastasis. After being sacrificed on day 21, the lung tissues were removed (Fig. 9A) and perfomed by histological assay. As a result, the lung/total weight and tumor nodules were obviously reduced after treatment with Cur (100, 200, and 300 mg/kg) (Fig. 9B). Histological examination (H&E) results indicated
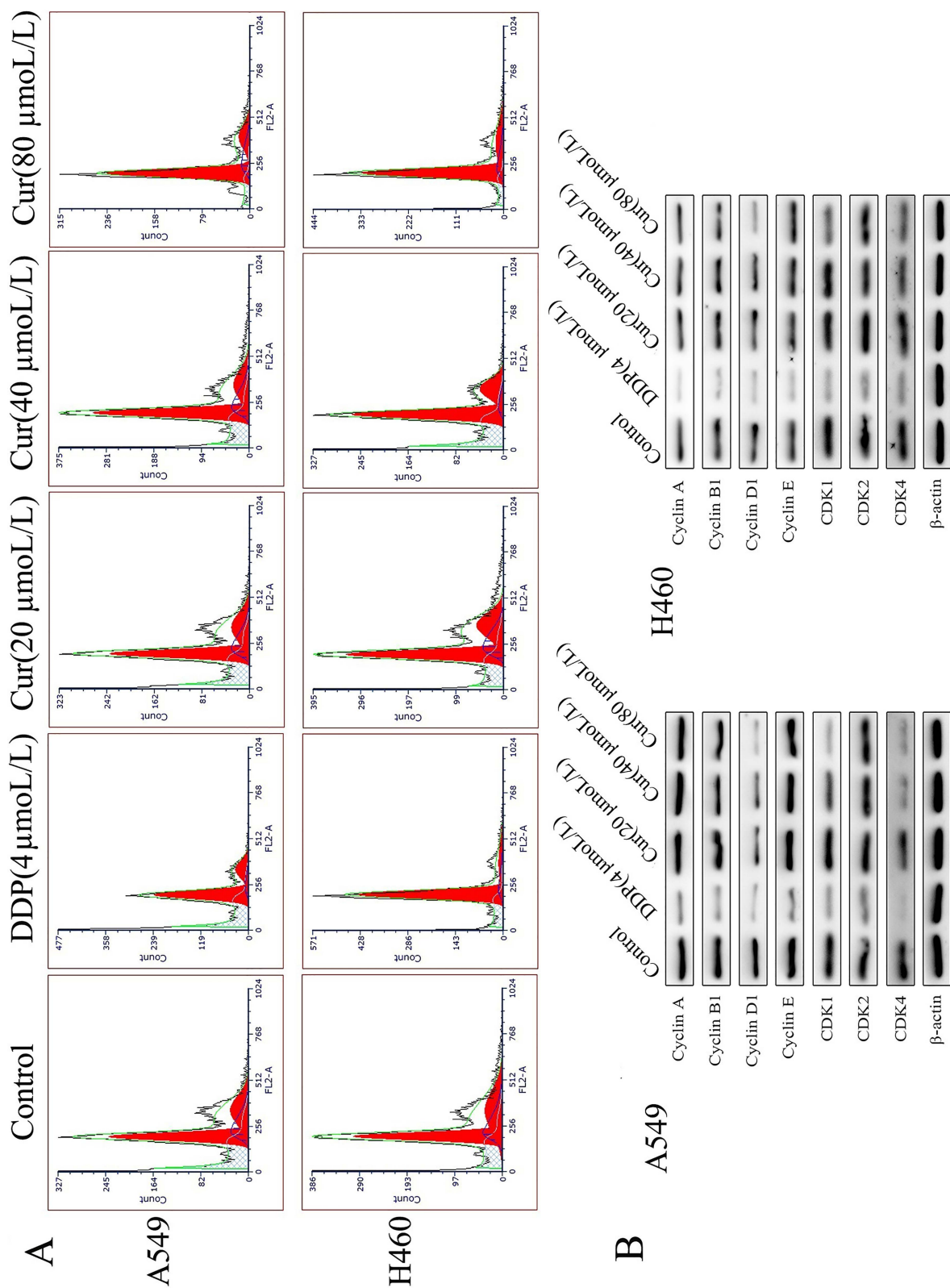
Figure 3. Effect of Cur on cell cycle phase distribution in A549 and H460 cells. (A) Cells were treated with Cur (20, 40, and 80 µmol/L) for 24 h, stained with propidium iodide (PI), and analyzed by flow cytometry (200×). (B) The expression of cyclin A, cyclin B1, cyclin D1, cyclin E, CDK1, CDK2, and CDK4 involved in cell cycle was analyzed by Western blotting. Cells were treated with Cur for 24 h, and total proteins were extracted. Equal protein loading was evaluated by β-actin.
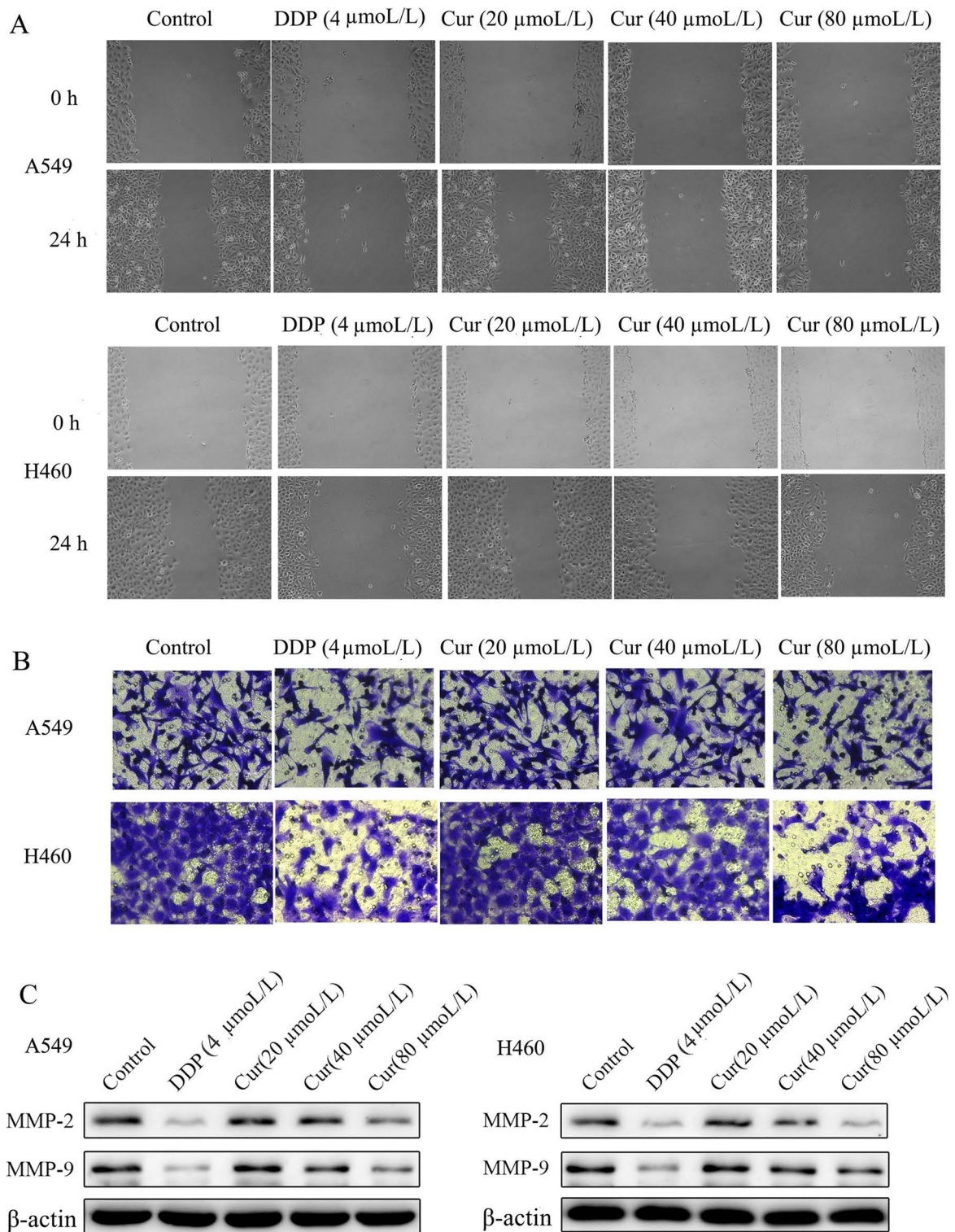
Figure 4. Inhibitory effect of Cur on A549 and H460 cell migration and invasion. Migration ability was determined by scratch wound assay (A), and invasive ability was determined by Transwell assay (B), and photographed at 200× magnification. (C) Western blot analysis of MMP-2 and MMP-9 in A549 and H460 cells treated with Cur (20, 40, and 80 µmol/L) for 24 h, and -actin was used as loading control.
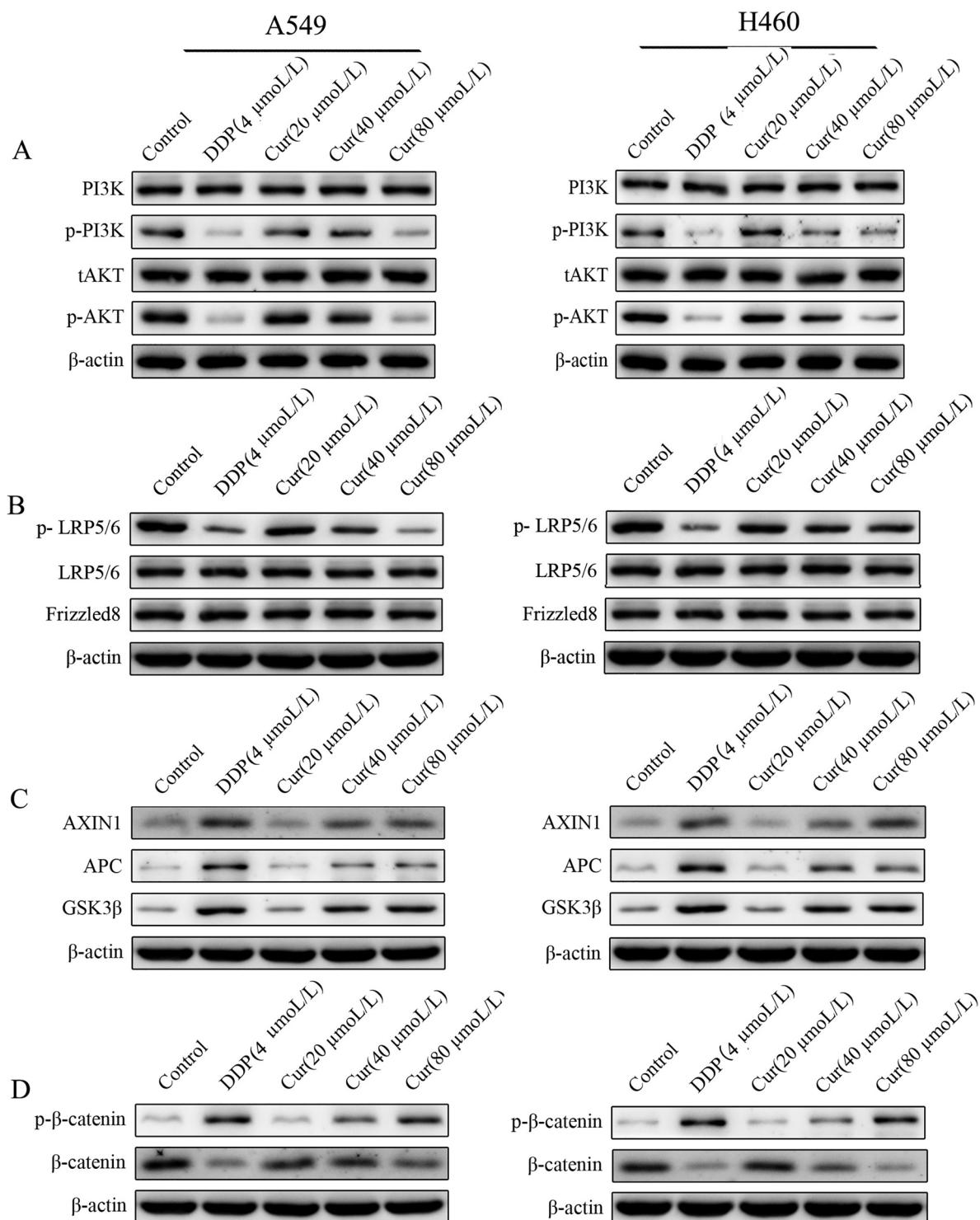
Figure 5. Cur regulated the PI3K/AKT and Wnt/ -catenin signaling proteins in A549 and H460 cells by Western blot analysis. (A) PI3k and AKT and their phosphorylation levels. (B) Cell membrane proteins (P-LRP, LRP, and Frizzled8) and (C) cell cytoplasm proteins (Axin1, APC, and GSK3) in Wnt signaling pathway. (D) The expression of p- -catenin and -catenin. A549 and H460 cells treated with Cur (20, 40, and 80 μmol/L) for 24 h, and total proteins were extracted. -actin was used as loading control.
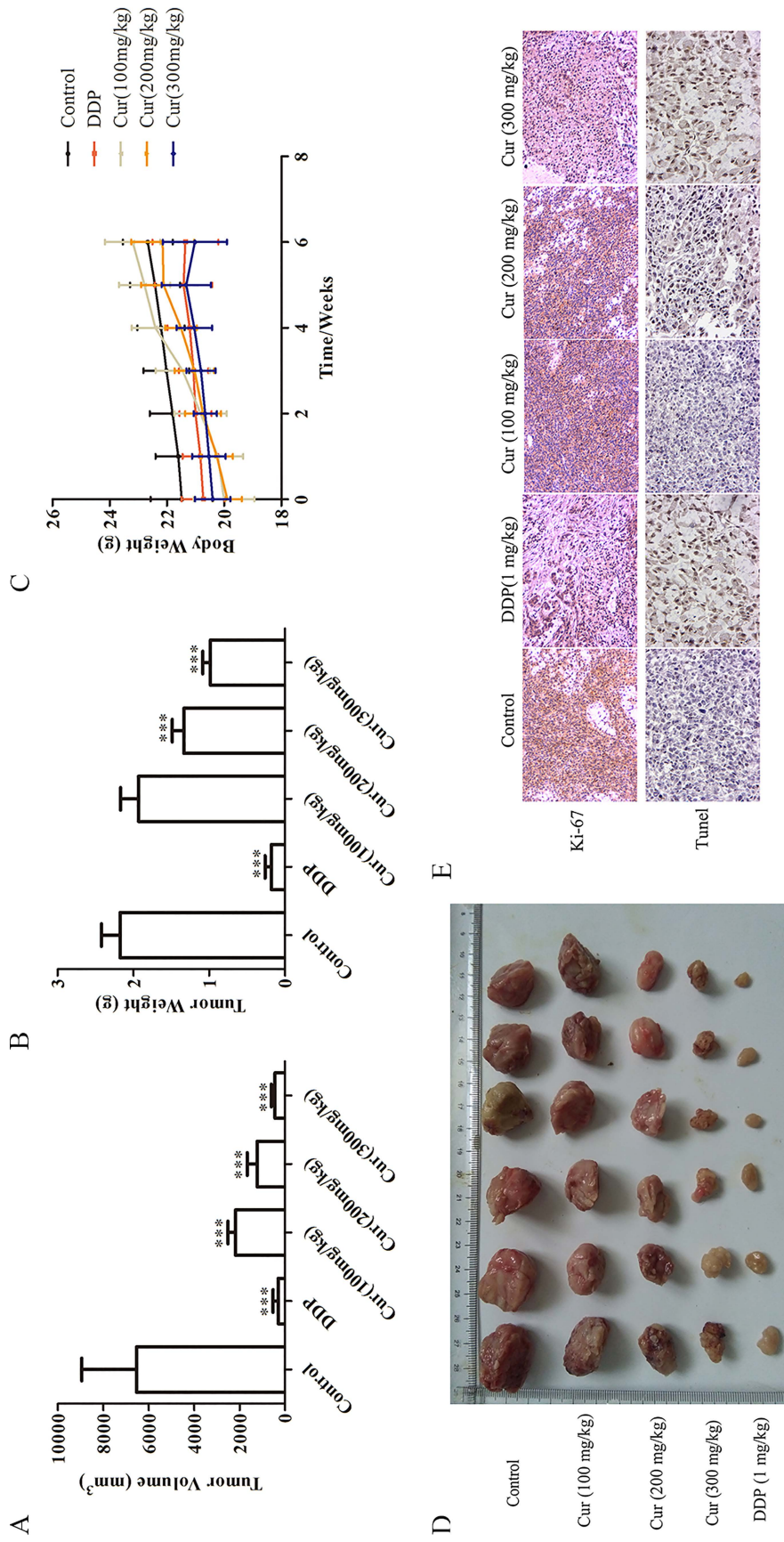
Figure 6. Cur suppressed the tumor growth in BALB/c nude mice. Mice were inoculated with A549 for 4 weeks prior to p.o. of 100, 200, and 300 mg/kg Cur and cisplatin (DDP) (1 mg/kg) dissolved in component solvent once a day for 21 days. (A) Tumor volume; (B) tumor weight; (C) body weight loss; (D) morphology of tumor; (E) immunohistochemistry of Ki-67 staining and TUNEL of xenografts tumor in the tumor sections (200×). Data are shown as the mean±SD ($n=6$). $*p<0.05$ and $**p<0.01$ versus control group.
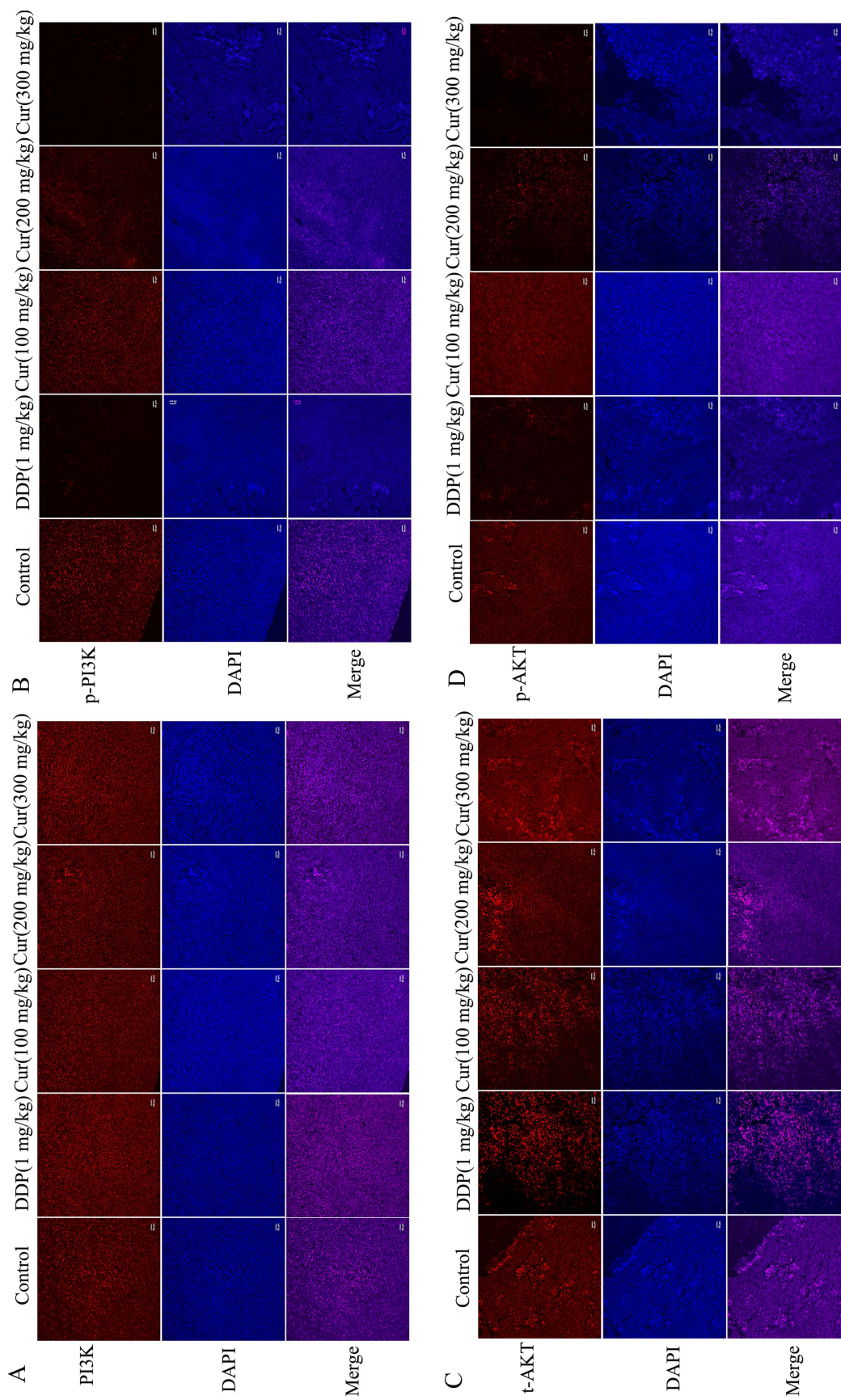
Figure 7. Effect of Cur on the level of PI3K (A), p-PI3K (B), t-AKT (C), and p-AKT (D) in lung tissues of tumor growth nude mice by immunofluorescence analysis (200×).
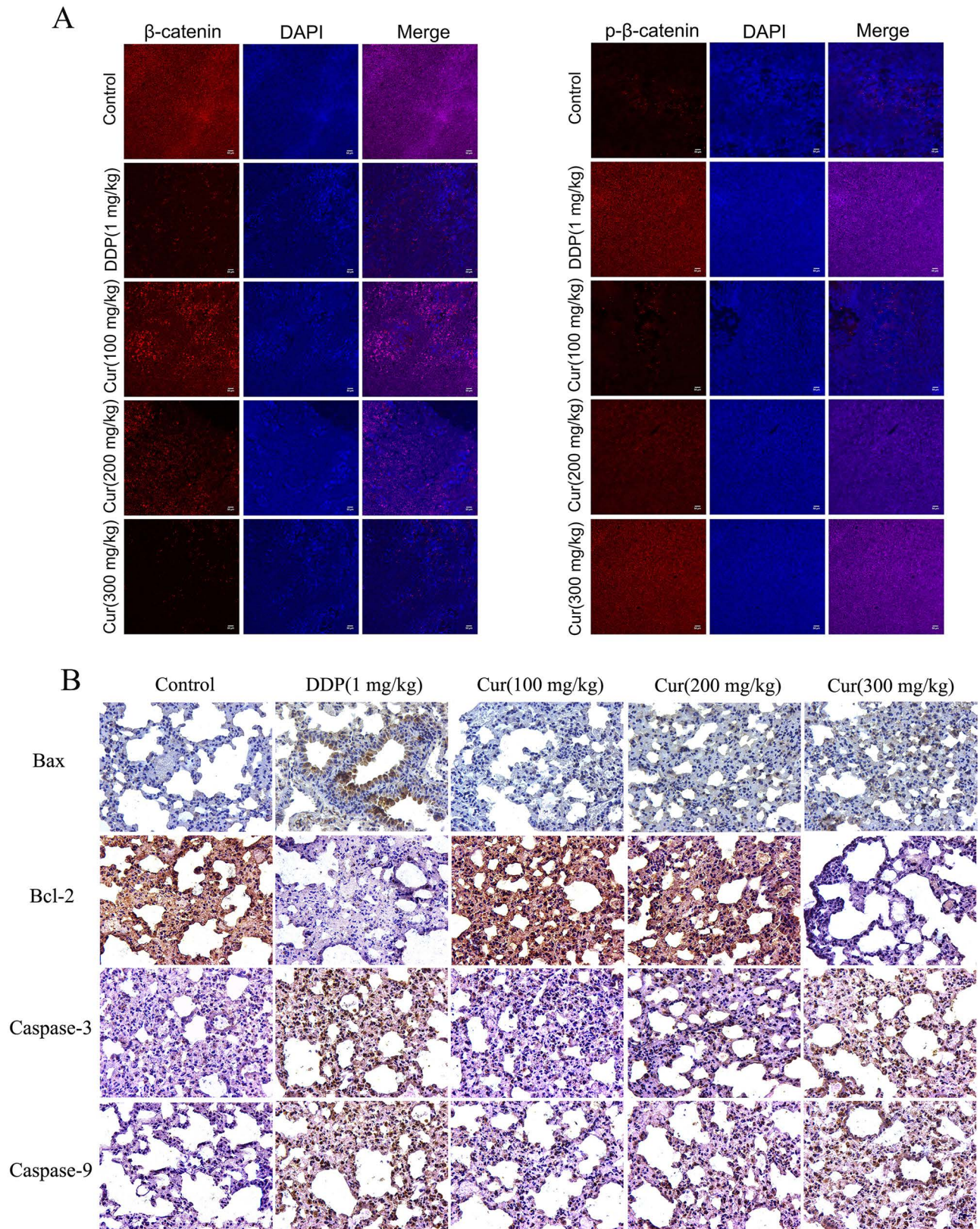
Figure 8. Effect of Cur on Wnt/ -catenin signaling (A) and Bax, Bcl-2, caspase 3, and caspase 9 protein (B) in lung tissues of tumor growth nude mice. The experimental lung tissue was studied by immunofluorescence analysis (200×).
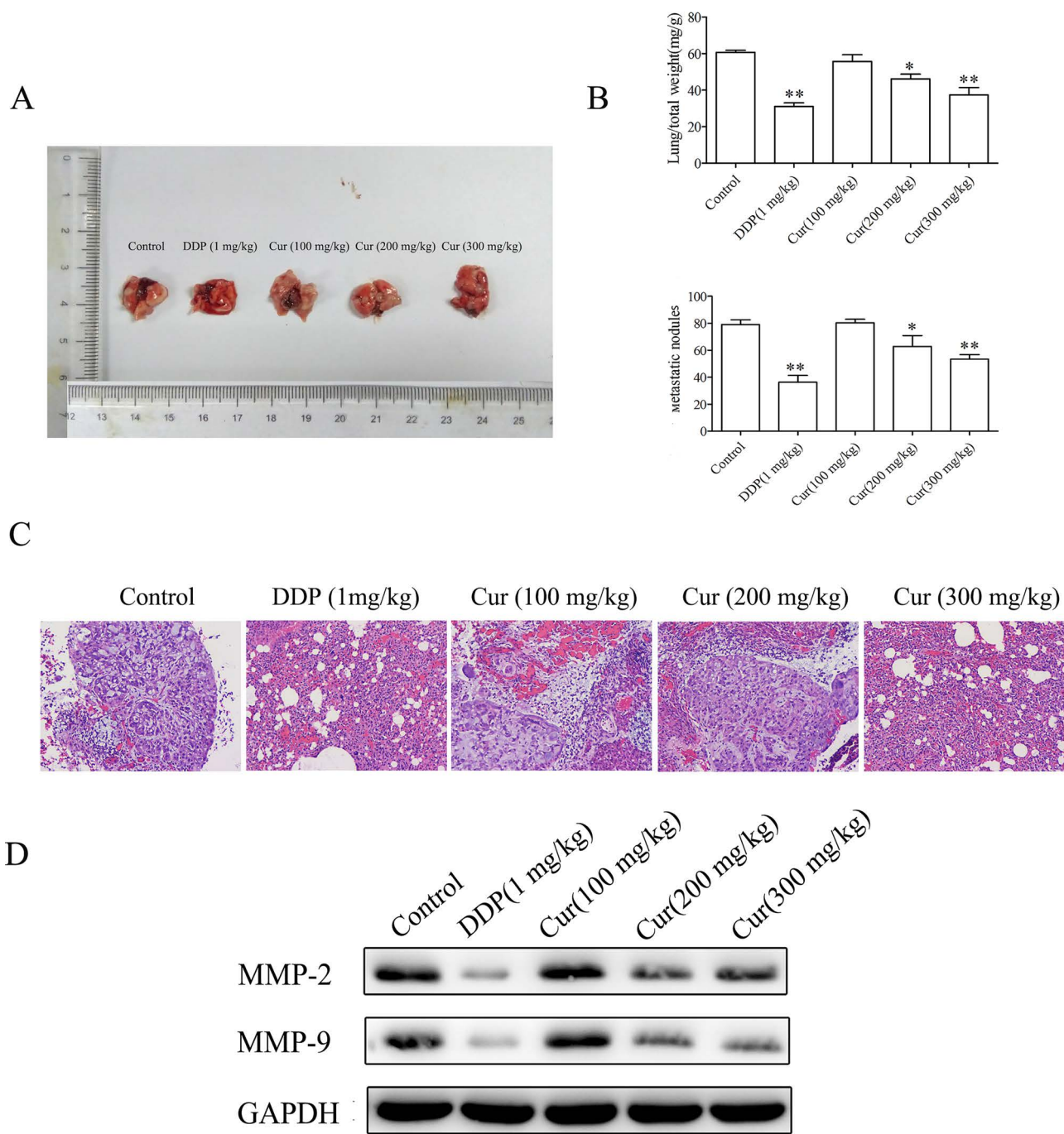
Figure 9. The effect of Cur on pulmonary metastasis in nude mice. (A) The representative pictures of lung size were photographed. (B) Lung/total weight and tumor nodules were measured. (C) The tissue sections were stained with H&E (200×). (D) Western blotting of MMP-2 and MMP-9 proteins of tumor specimen from the pulmonary metastasis nude mice. Equal protein loading was evaluated by -actin. Data are shown as the mean±SD ($n=6$). *$p<0.05$ and **$p<0.01$ versus control group.

that there are lower metastases in Cur treatment groups (Fig. 9C). Furthermore, Cur (100, 200, and 300 mg/kg) groups showed lower expression of MMP-2 and MMP-9, compared with controls (Fig. 9D). Collectively, these results provided the some evidence to support the hypothesis that Cur could suppress tumor metastasis in mice.

DISCUSSION

At present, more and more studies have found the important role of natural medicines' chemical compounds originating from plant extracts for treatment of human disease[23]. It is an efficient therapeutic method for the treatment of metastatic tumors by targeting natural products[24–26]. In this study, we found that curcumol (Cur) suppressed lung adenocarcinoma cells (A549 and H460) both in vitro and in vivo as the expression of antiproliferative, apoptosis inducible, antimigration, anti-invasion, and antimetastasis, and these effects maybe mediated by inhibiting the PI3K/AKT and Wnt/ -catenin pathways.

Tumor spreading to cancer to bones, lungs, and brain is largely dependent on the ability of tumor cells to invade the adjacent tissues, which also successfully establishes a metastatic tumor. Therefore, prevention of cancer cell metastasis is an effective strategy for successful management of cancers. Cur has been reported to be effective against multiple conditions, particularly cancers[27–29]. To date, the mechanisms of Cur on lung cancer metastasis have been poorly understood. We found that Cur inhibited cell proliferation, migration, and invasion, promoted cell apoptosis, and arrested the cell cycle in two lung cancer cell lines. These results were related to the signaling molecules regulating several tumor properties including proliferation (p-AKT, p-PI3K, p-LRP5/6, AXIN, APC, GSK3 , and p- -catenin), migration and invasiveness (MMP-2 and MMP-9), apoptosis (Bax, Bcl-2, caspase 3, and caspase 9), and cell cycle (cyclin D1, CDK1, and CDK4). These data indicate that Cur possesses significant antiproliferation and antimetastatic properties against lung cancer cells in vitro.

Pathways in cancer represent a comprehensive network of the integration of all pathways related to tumorigenesis and cancer progression, such as PI3K–AKT, MAPK, WNT, Wnt/ -catenin, and other pathways associated with cancer cell proliferation, invasion, and metastasis[21,30]. Using a database, we confirmed that PI3K/AKT and Wnt/ -catenin could regulate the cell proliferation and survival, motility and migration, apoptosis, and invasion[31,32]. A recognized hallmark of cancer cell survival and growth is an aberrant activation of growth signaling pathways including Wnt, which has become a valid target in antitumor therapy[33–35]. Western blot and immunofluorescence analysis showed that Cur downregulated the expression of p-PI3K and p-AKT, and reduced PI3K/

AKT nuclear translocation (Figs. 5A and 7). In addition, Cur negatively regulated the Wnt/ -catenin pathway by suppressing p-LRP5/6, in turn increasing AXIN, APC, and GSK3 protein expression to inhibit the expression and nuclear translocation of -catenin (Figs. 5B–D and 8A). Importantly, the current study is the first demonstration that antiproliferation and antimetastatic activity of Cur is mediated through modulation of PI3K/AKT and Wnt/ -catenin activity.

The in vitro studies have shown that Cur has notable antiproliferation/antimetastasis activities. The results of in vivo studies are consistent with in vitro data. Ki-67 monoclonal antibody detects only the nuclear antigen in proliferating cells. Cur treatment significantly decreased Ki-67 expression in tumors, which confirmed that Cur could inhibit osteosarcoma cell proliferation in vivo. Developing more effective drugs to aberrant cell proliferation and apoptosis has been one of the promising chemotherapeutic strategies[21,36]. Here, Cur increased nuclear TUNEL staining, controlled proapoptotic Bax and antiapoptotic Bcl-2 proteins (Figs. 6F and 8). Besides, PI3K/AKT and Wnt/ -catenin inhibition by Cur suppressed lung cancer cell proliferation and metastasis in a mice model (Figs. 7 and 8). Our in vivo results are also consistent with studies on other tumor types, including melanoma, prostate, pancreas, and glioma cancer, where inhibition of FAK kinase activity results in inhibition of tumor metastasis[37–39]. Effects of PI3K/AKT and Wnt/ -catenin inhibition may be attributed to modest inhibition of tumor procedure.

Taken together, our data demonstrated the antiproliferative and antimetastatic effect of curcumol in vitro and in vivo. These inhibitory effects are mediated through inhibition of PI3K/AKT and Wnt/ -catenin, supporting therapeutic approaches targeting PI3K/AKT and Wnt/ -catenin activity to prevent lung adenocarcinoma development and tumor metastasis.

REFERENCES

1. Siegel R, Naishadham D, Jemal A. Cancer statistics. CA Cancer J Clin. 2013;63(1):11–30.
2. Devarakonda S, Morgensztern D, Govindan R. Genomic alterations in lung adenocarcinoma. Lancet Oncol. 2015;16(7):e342–51.
3. Mitsudomi T, Morita S, Yatabe Y, Negoro S, Okamoto I, Tsurutani J, Seto T, Satouchi M, Tada H, Hirashima T, Asami K, Katakami N, Takada M, Yoshioka H, Shibata K, Kudoh S, Shimizu E, Saito H, Toyooka S, Nakagawa K, Fukuoka M; West Japan Oncology Group. Gefitinib versus cisplatin plus docetaxel in patients with non-small-cell lung cancer harbouring mutations of the epidermal growth factor receptor (WJTOG3405): An open label, randomised phase 3 trial. Lancet Oncol. 2010;11(2):121–8.

4. Kumar MS, Hancock DC, Molina-Arcas M, Steckel M, East P, Diefenbacher M, Armenteros-Monterroso E, Lassailly F, Matthews N, Nye E, Stamp G, Behrens A, Downward J. The GATA2 transcriptional network is requisite for RAS oncogene-driven non-small cell lung cancer. Cell 2012;149(3):642–55.

5. Aupérin A, Le Péchoux C, Rolland E, Curran WJ, Furuse K, Fournel P, Belderbos J, Clamon G, Ulutin HC, Paulus R, Yamanaka T, Bozonnat MC, Uitterhoeve A, Wang X, Stewart L, Arriagada R, Burdett S, Pignon JP. Meta-analysis of concomitant versus sequential radiochemotherapy in locally advanced non-small-cell lung cancer. J Clin Oncol. 2010;28(13):2181–90.

6. Travis WD. Pathology of lung cancer. Clin Chest Med. 2011;32(4):669–92.

7. Govindan R, Ding L, Griffith M, Subramanian J, Dees ND, Kanchi KL, Maher CA, Fulton R, Fulton L, Wallis J, Chen K, Walker J, McDonald S, Bose R, Ornitz D, Xiong D, You M, Dooling DJ, Watson M, Mardis ER, Wilson RK. Genomic landscape of non-small cell lung cancer in smokers and never-smokers. Cell 2012;150(6):1121–34.

8. Chow SC, Gowing SD, Cools-Lartigue JJ, Chen CB, Berube J, Yoon HW, Chan CH, Rousseau MC, Bourdeau F, Giannias B, Roussel L, Qureshi ST, Rousseau S, Ferri LE. Gram negative bacteria increase non-small cell lung cancer metastasis via Toll-like receptor 4 activation and mitogen-activated protein kinase phosphorylation. Int J Cancer 2015;136(6):1341–50.

9. Zaba O, Grohe C, Merk J. Novel therapies in non-small cell lung cancer. Minerva Chir. 201;66(3):235–44.

10. Acunzo M, Visone R, Romano G, Veronese A, Lovat F, Palmieri D, Bottoni A, Garofalo M, Gasparini P, Condorelli G, Chiariello M, Croce CM. miR-130a targets MET and induces TRAIL-sensitivity in NSCLC by downregulating miR-221 and 222. Oncogene 2012;31(5):634–42.

11. Sawabata N, Okumura M, Utsumi T, Inoue M, Shiono H, Minami M, Nishida T, Sawa Y. Circulating tumor cells in peripheral blood caused by surgical manipulation of non-small-cell lung cancer: Pilot study using an immunocytology method. Gen Thorac Cardiovasc Surg. 2007;55(5):189–92.

12. Kratz JR, He J, Van Den Eeden SK, Zhu ZH, Gao W, Pham PT, Mulvihill MS, Ziaei F, Zhang H, Su B, Zhi X, Quesenberry CP, Habel LA, Deng Q, Wang Z, Zhou J, Li H, Huang MC, Yeh CC, Segal MR, Ray MR, Jones KD, Raz DJ, Xu Z, Jahan TM, Berryman D, He B, Mann MJ, Jablons DM. A practical molecular assay to predict survival in resected non-squamous, non-small-cell lung cancer: Development and international validation studies. Lancet 2012;379(9818):823–32.

13. Lee H, Baek SH, Lee JH, Kim C, Ko JH, Lee SG, Chinnathambi A, Alharbi SA, Yang WM, Um JY, Sethi G, Ahn KS. Isorhynchophylline, a potent plant alkaloid, induces apoptotic and anti-metastatic effects in human hepatocellular carcinoma cells through the modulation of diverse cell signaling cascades. Int J Mol Sci. 2017;18(5):1095.

14. Lee TK, Roh HS, Yu JS, Baek J, Lee S, Ra M, Kim SY, Baek KH, Kim KH. Pinecone of Pinus koraiensis inducing apoptosis in human lung cancer cells by activating caspase-3 and its chemical constituents. Chem Biodivers. 2017;14(4).

15. Carey AN, Fisher DR, Rimando AM, Gomes SM, Bielinski DF, Shukitt-Hale B. Stilbenes and anthocyanins reduce stress signaling in BV-2 mouse microglia. J Agric Food Chem. 2013;61(25):5979–86.

16. Wang J, Huang F, Bai Z, Chi B, Wu J, Chen X. Curcumol inhibits growth and induces apoptosis of colorectal cancer LoVo cell line via IGF-1R and p38 MAPK Pathway. Int J Mol Sci. 2015;16(8):19851–67.

17. Ning L, Ma H, Jiang Z, Chen L, Li L, Chen Q, Qi H. Curcumol suppresses breast cancer cell metastasis by inhibiting MMP-9 via JNK1/2 and Akt-dependent NF- B signaling pathways. Integr Cancer Ther. 2016;15(2):216–25.

18. Chen DL, Wang ZQ, Zeng ZL, Wu WJ, Zhang DS, Luo HY, Wang F, Qiu MZ, Wang DS, Ren C, Wang FH, Chiao LJ, Pelicano H, Huang P, Li YH, Xu RH. Identification of microRNA-214 as a negative regulator of colorectal cancer liver metastasis by way of regulation of fibroblast growth factor receptor 1 expression. Hepatology 2014;60(2):598–609.

19. Gao TY, Jin X, Tang WZ, Wang XJ, Zhao YX. New geranylated flavanones from the fruits of Paulownia catalpifolia Gong Tong with their anti-proliferative activity on lung cancer cells A549. Bioorg Med Chem Lett. 2015;25(17):3686–9.

20. Sui Y, Li S, Shi P, Wu Y, Li Y, Chen W, Huang L, Yao H, Lin X. Ethyl acetate extract from Selaginella doederleinii Hieron inhibits the growth of human lung cancer cells A549 via caspase-dependent apoptosis pathway. J Ethnopharmacol. 2016;190:261–71.

21. Fang Y, Zhang C, Wu T, Wang Q, Liu J, Dai P. Transcriptome sequencing reveals key pathways and genes associated with cisplatin resistance in lung adenocarcinoma A549 cells. PLoS One 2017;12(1):e0170609.

22. Hanahan D, Weinberg RA. Hallmarks of cancer: The next generation. Cell 2011;144(5):646–74.

23. Park MN, Song HS, Kim M, Lee MJ, Cho W, Lee HJ, Hwang CH, Kim S, Hwang Y, Kang B, Kim B. Review of natural product-derived compounds as potent antiglioblastoma drugs. Biomed Res Int. 2017;2017:8139848.

24. Wei Z, Shan Y, Tao L, Liu Y, Zhu Z, Liu Z, Wu Y, Chen W, Wang A, Lu Y. Diallyl trisulfides, a natural histone deacetylase inhibitor, attenuate HIF-1 synthesis, and decreases breast cancer metastasis. Mol Carcinog. 2017;56(10):2317–31.

25. Silva IT, Geller FC, Persich L, Dudek SE, Lang KL, Caro MS, Durán FJ, Schenkel EP, Ludwig S, Simões CM. Cytotoxic effects of natural and semisynthetic cucurbitacins on lung cancer cell line A549. Invest New Drugs 2016;34(2):139–48.

26. Wang X, Lao Y, Xu N, Xi Z, Wu M, Wang H, Li X, Tan H, Sun M, Xu H. Oblongifolin C inhibits metastasis by up-regulating keratin 18 and tubulins. Sci Rep. 2015;5:10293.

27. Zhang J, Su G, Tang Z, Wang L, Fu W, Zhao S, Ba Y, Bai B, Yue P, Lin Y, Bai Z, Hu J, Meng W, Qiao L, Li X, Xie X. Curcumol exerts anticancer effect in cholangiocarcinoma cells via down-regulating CDKL3. Front Physiol. 2018;9:234.

28. Zhang N, Yu S, Liu X, Lu H. Low dose of lipopolysaccharide pretreatment preventing subsequent endotoxin-induced uveitis is associated with PI3K/AKT Pathway. J Immunol Res. 2017;2017:1273940.

29. Huang L, Li A, Liao G, Yang F, Yang J, Chen X, Jiang X. Curcumol triggers apoptosis of p53 mutant triple-negative human breast cancer MDA-MB 231 cells via activation of p73 and PUMA. Oncol Lett. 2017;14(1):1080–8.

30. Zhang C, Wang LM. Inhibition of autophagy attenuated curcumol-induced apoptosis in MG-63 human osteosarcoma cells via Janus kinase signaling pathway. Oncol Lett. 2017;14(6):6387–94.

31. Xue M, Ji X, Xue C, Liang H, Ge Y, He X, Zhang L, Bian K, Zhang L. Caspase-dependent and caspase-independent induction of apoptosis in breast cancer by fucoidan via the PI3K/AKT/GSK3 pathway in vivo and in vitro. Biomed Pharmacother. 2017;94:898–908.

32. Lee CY, Kuo WW, Baskaran R, Day CH, Pai PY, Lai CH, Chen YF, Chen RJ, Padma VV, Huang CY. Increased -catenin accumulation and nuclear translocation are associated with concentric hypertrophy in cardiomyocytes. Cardiovasc Pathol. 2017;31:9–16.

33. Clevers H. Wnt/beta-catenin signaling in development and disease. Cell 2006;127(3):469–80.

34. Hong CF, Chen WY, Wu CW. Upregulation of Wnt signaling under hypoxia promotes lung cancer progression. Oncol Rep. 2017;38(3):1706–14.

35. Tai D, Wells K, Arcaroli J, Vanderbilt C, Aisner DL, Messersmith WA, Lieu CH. Targeting the WNT signaling pathway in cancer therapeutics. Oncologist 2015;20(10): 1189–98.

36. Sak K. Cytotoxicity of dietary flavonoids on different human cancer types. Pharmacogn Rev. 2014;8(16):122–46.

37. Ju H, Li Y, Xing X, Miao X, Feng Y, Ren Y, Qin J, Liu D, Chen Z, Yang Z. Manganese-12 acetate suppresses the migration, invasion, and epithelial-mesenchymal transition by inhibiting Wnt/ -catenin and PI3K/AKT signaling pathways in breast cancer cells. Thorac Cancer. 2018;9(3):353–9.

38. Ko JK, Auyeung KK. Target-oriented mechanisms of novel herbal therapeutics in the chemotherapy of gastrointestinal cancer and inflammation. Curr Pharm Des. 2013;19(1):48–66.

39. Gajos-Michniewicz A, Czyz M. Modulation of WNT/ -catenin pathway in melanoma by biologically active components derived from plants. Fitoterapia 2016;109: 283–92.